Supporting Information

Bruss and Grason 10.1073/pnas.1205606109

SI Text

Algorithm for Asymptotically Close-Packed Bundles. Here, we describe the deterministic algorithm used to construct the core packing of asymptotically close-packed twisted bundles. This algorithm proceeds by sequentially adding new filaments to an existing cluster of close-packed filaments. In essence, it is based on Rubinstein and Nelson's 2D generalization (1, 2) of Bennett's algorithm of close-packed clusters of spheres in 3D (3). Given a cluster of close-packed filaments, the algorithm proceeds as follows. First, it searches for all available pockets of close contact on the surface of the cluster. A pocket is defined by the position of a filament center that is in contact with two filaments of the cluster (where contact is defined by the condition $\Delta_* = d$) and that is nonoverlapping ($\Delta_* \geq d$) for all other filaments in the cluster. After the list of available pockets is tabulated, a new filament is added to the cluster in the pocket furthest from the bundle center. The algorithm repeats until the core the bundle has no available filament pockets.

To generate bundle packings that are asymptotically dense, we seed the packing with an initial "collar" of filaments at a large radius, which is consistent with the hexagonal symmetry of close packed at $\rho \to \infty$. To construct this collar, we exploit the fact that the metric geometry of bundles becomes nearly Euclidean, with the topology of a cylinder, far from the bundle core $\Omega\rho \gg 1$. The integer pair (n, m) defines the wrapping vector, $\mathbf{P}(n, m)$, as in Eq. **10**. As shown in Fig. S1, starting from an initial position in the hexagonal lattice of spacing d, n disks are arrayed along the lattice vector $\mathbf{a}_1$ followed by m disks arrayed along the lattice vector $\mathbf{a}_2$. Identifying the first and last lattice position in this sequence, separated by the vector $\mathbf{P}(n, m)$, the array of $n + m$ disks is rolled up along $\mathrm{P}(n, m)$ into a collar encircling a cylindrical surface (see Fig. S1). Placing the initial disk at an arc distance, $5P + \delta\rho$ from the pole of the bundle-equivalent dome, the radial and angular positions of disks in the collar are used to define the initial cluster of filaments in the packing. The value of $\delta\rho$ is discussed below. We assume that the packing maintains the hexagonal geometry of the initial collar for filaments further from the core, so that regions outside of this collar are fully packed, and further filaments are only added at positions within this initial collar until the core is fully occupied.

To measure the density of packing within the core of the bundle, defined to be a region within a radial distance $\rho_{\mathrm{core}} = 3P$ from the bundle center, we calculate the occupied area within the filament cross-sections in this central region, $A(\rho_{\mathrm{core}})$. The volume fraction of the core is simply $\Phi(\rho_{\mathrm{core}}) = A(\rho_{\mathrm{core}})/\pi\rho_{\mathrm{core}}^2$. Because of periodic oscillations in the number of filaments intersected by the core boundary, the value of area (or volume) fraction is highly sensitive to the value of ρ_{core}, exhibiting oscillations on length scales corresponding to the periodic symmetry of the packing far from the core (as shown in Fig. S1). To construct a measure of packing fraction less sensitive to the well-packed structure at the boundary of the core, we define the packing fraction as the average of $\Phi(\rho_{\mathrm{core}})$ over the narrow range of core radii $3P - \delta/2 < \rho_{\mathrm{core}} < 3P + \delta/2$,

$$\Phi = \frac{1}{\delta}\int_{-\delta/2}^{\delta/2} d\rho_{\mathrm{core}}\Phi(\rho_{\mathrm{core}}), \qquad \textbf{[S1]}$$

where $\delta = d\sin(\psi + \pi/3)$ defines a radial shift of the packing consistent with the hexagonal symmetry of asymptotic close packing. Here, $\sin\psi = |n\mathbf{a}_1 \times m\mathbf{a}_2|$, as shown in Fig. S1. Fig. S2 shows that this definition of packing fraction varies smoothly with the core radius, providing a more robust measure of packing efficiency in the bundle.

Given the initial collar configuration, the packing algorithm fills the core via a deterministic sequence of filament additions. However, whereas the packing density of the bundle outside of the collar is degenerate with respect to changes of initial radial position of the collar filaments, the core packing structure of the bundle is highly sensitive to shifts in $\delta\rho$. Thus, for a given integer pair (n, m), the packing algorithm is repeatedly performed with the initial collar position shifted over a narrow range $-\delta/2 < \delta\rho < +\delta/2$. The optimal packing geometry corresponds to the largest value of Φ achieved for this sequence of collar radii.

Triangulation of Twisted Bundle Packings. Interfilament distance in twisted bundles is not preserved when the cross-sectional packing is projected into the plane (as in a horizontal cross-section of the bundle shown in Fig. S1), and hence, determination of the nearest-neighbor bond network requires some care. A very efficient and sufficiently accurate method is to map the filament positions onto the plane via a coordinate transformation that rescales local interfilament distances in different directions (radially and azimuthally) by nearly equivalent amounts and then perform the standard planar Delaunay triangulation on the transformed array. That is, we use the isothermal coordinate map of filament position (ρ, ϕ) in the horizontal section to position $(\bar{\rho}, \phi)$ in the plane. Such transformation is conformal and, as a consequence, it maps infinitesimal circles on the dome to circles in the plane. For sufficiently small, but finite-size, circles (i.e., $d/P \lesssim 1$), the Delaunay triangulation of the mapped positions will give the identical connectivity of nearest neighbors as a triangulation based on true geodesic distances on the bundle-equivalent dome.

The coordinate transformation is described by the function $\bar{\rho}(\rho)$ that transforms twisted bundle metric of Eq. **5** into the following form,

$$ds^2 = \omega^2(\bar{\rho})(d\bar{\rho}^2 + \bar{\rho}^2 d\phi^2), \qquad \textbf{[S2]}$$

where $\omega(\bar{\rho})$ describes the conformal scaling of area elements. This transformation satisfies

$$\bar{\rho}\frac{\partial\bar{\rho}}{\partial\rho} = \Omega^{-1}\sin\theta(\rho), \qquad \textbf{[S3]}$$

from which we find

$$\bar{\rho} = \frac{\rho}{1 + \sqrt{1 + (\Omega\rho)^2}}\, e^{\sqrt{1+(\Omega\rho)^2}}, \qquad \textbf{[S4]}$$

and $\omega(\rho) = [1 + \cos\theta(\rho)]e^{\sec\theta(\rho)}$. In Fig. S3, we show the planar section of a $(5, 5)$ bundle as well as the conformal transform of the cross-section and corresponding triangulation. Note that, for this bundle, $d/P = 0.12$, so that filament cross-sections are very nearly circular in the projection.

Energy Minimization of Self-Assembled Twisted Filament Bundles. Here, we detail the protocol for numerically minimizing the energy of adhesive filament bundles. For a given filament number, N and helical twist, Ω, every minimization was initialized with a random distribution of filament positions in the 2D plane. Given the in-plane coordinates of all filaments, the in-plane gradients of the total energy with respect to filament positions (the forces) are calculated making use of the analytical approximation for

vertical offset of close contact, or z_*, given in [**12**]. The algorithm updates the positions of every filament via steepest descent, and recalculates the forces at each step. To keep the center of rotation at the geometric center of the bundle, the total force acting on the center of mass of the cross-section is removed from the update, and the center of mass remains at the $\mathbf{x} = 0$ center of rotation.

Because of the many mechanically stable local minimal energy of twisted filament clusters, we augmented the steepest-descent method with a specialized annealing step that systematically redistributes filaments in an attempt to fill in internal voids that are a common feature in the initially quenched structures. In this routine, after a minima is reached by standard steepest decent, a high-energy filament along the outer edge of the bundle is moved to fill a potential void. The system is then allowed to relax again and, if the new final energy is lower, the move is kept, else it is undone. This process is repeated until all potentially unfavorable voids are filled. For the purposes of efficiency, interfilament forces are truncated beyond a cutoff distance of $4d$. Interfilament forces are implemented via a Verlet neighbor list, which is completely regenerated after any filament has moved a maximum of $1d$. Once a suitable minima is reached, the interaction cutoff is removed for the final relaxation step.

We find the number of local energy minima appears to grow exponentially with the system size, a feature seemingly common among systems that include defects in their lowest energy packings, such as the Thomson problem, where repulsive particles are packed on the surface of a sphere (4). To overcome this complication, a large number of copies of the same simulations (with constant N and Ω) are performed with different random initial configurations. The exact number of copies is set to increase exponentially with system size from 300 (for $N = 16$) to 2,000 (for $N = 100$). All simulations with $N \geq 100$ were run at a maximum of 2,000 copies. The complexity of the energy landscape can be seen in Fig. S4, which shows the distribution of local energy minima resolved by the algorithm for a particular bundle size and twist. Given the huge number of the minima in the complex energy landscape of a large twisted bundle, it is possible that even the larger number (approximately 10^3) of initial configurations used here is insufficient to resolve absolute lowest global energy states (especially for large N). Notwithstanding the unavoidable roughness of the ground-state manifold of frustrated crystals, we find that all states within a neighborhood of the global minima are characterized by equal, or nearly equal, geometry as measured by Q and R, total disclination charge and bundle radius, respectively. Thus, with the number of simulated quenches used here for a given bundle size and twist, we obtain multiple "nearly minimal-energy" filament packings that nevertheless accurately represent the geometry of the true global energy minimum.

Final simulation results are subject to a Delaunay triangulation of the isothermal coordinate map of the filament positions (described above). This triangulation method always produces a bond network with a convex boundary of bonds encompassing the entire bundle. However, in many cases, this triangulation includes extra-long bonds that bridge naturally concave sections of the hull. Because these bonds exist as an artifact of the triangulation and not as a product of the governing interaction energy, bonds along the boundary with $\Delta_* \geq 1.4d$ are removed from the triangulation. From this final triangulation, simulation results are then classified by their radius R/d, net disclination charge Q, and total disclination number. R was calculated to be the mean distance from the center of mass of every filament along the outer hull of the cross-section.

1. Rubinstein M, Nelson DR (1982) Order and deterministic chaos in hard-disks arrays. *Phys Rev B Condens Matter Mater Phys* 26:6254–6275.
2. Rubinstein M, Nelson DR (1983) Dense-packed arrays on surfaces of constant negative curvature. *Phys Rev B Condens Matter Mater Phys* 28:6377–6386.
3. Bennett CH (1972) Serially deposited amorphous aggregates of hard spheres. *J Appl Phys* 43:2727–2734.
4. Altschuler E, et al. (1997) Possible global minimum lattice configurations for Thomson's problem of charges on a sphere. *Phys Rev Lett* 78:2681–2685.

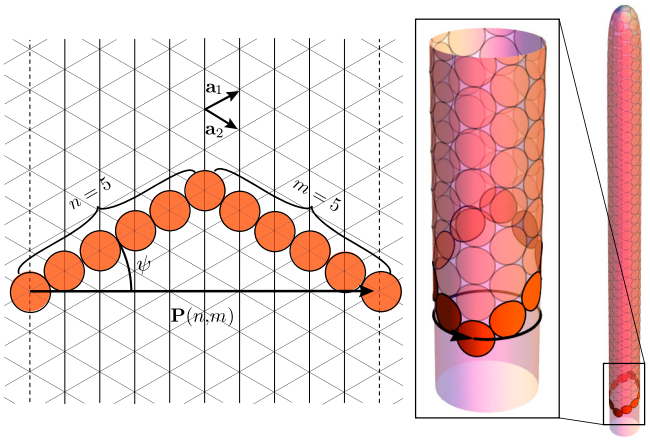

Fig. S1. (*Left*) The hexagonal packing in the initial collar used to seed the deterministic packing of the asymptotically closed-packed (n, m) structure. (*Right*) The packing indicates wrapping of the collar, described by vector, **P**, around the cylindrical geometry of the bundle-equivalent dome far from the core.

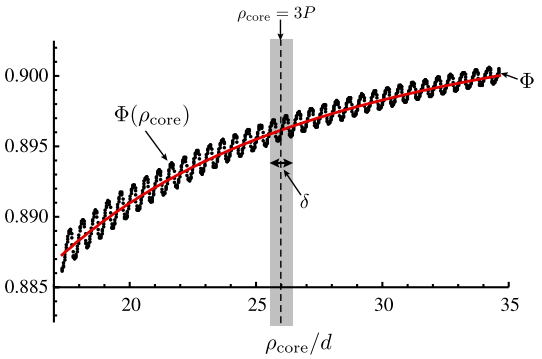

Fig. S2. The black data points show the value of core packing fraction vs. core radius for a $(5, 5)$ close-packed bundle. The short length scale, δ, modulations of $\Phi(\rho_{\text{core}})$ derive from periodicity of hexagonally packing in asymptotically dense regions. To achieve a measure of core density less sensitive to the intersection of boundary packing with the core radius, core fraction is averaged over the domain of core radii shown in gray. This boundary averaging leads to the red curve, which depicts the value of Φ given in Eq. **1** and used in our density calculations.

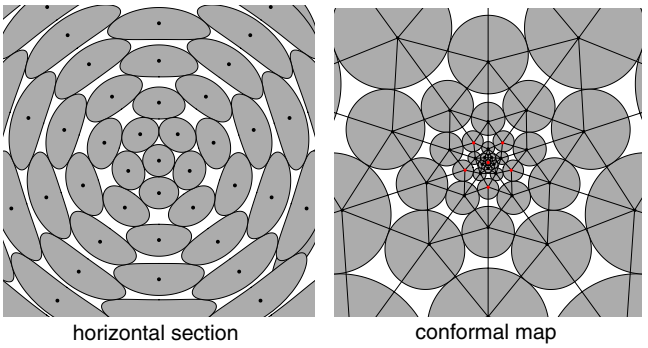

Fig. S3. On the left is shown the horizontal section of a $(5, 5)$ twisted bundle and, on the right, the conformal mapping of the that section described by Eq. **4** with the corresponding Delaunay triangulation connecting the mapped centerline positions.

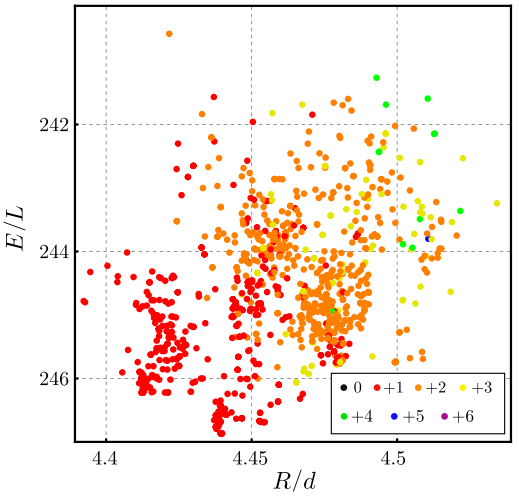

Fig. S4. Each data point is the result of simulated quenches with $N = 80$, $\Omega = 0.15$, and random initial starting filament locations. There are 1,000 simulations total, of which just six achieve the ground-state energy. Only the lowest energy result is retained for full analysis.